

Directionality-induced jamming in multiplex networks

Mateo Bouchet,^{1,2} Alejandro Tejedor,^{1,2,*} Xiangrong Wang,^{3,†} and Yamir Moreno^{1,2,‡}

¹*Institute for Biocomputation and Physics of Complex Systems (BIFI), Universidad de Zaragoza, 50018 Zaragoza, Spain*

²*Department of Theoretical Physics, University of Zaragoza, 50009 Zaragoza, Spain*

³*College of Mechatronics and Control Engineering, Shenzhen University, Shenzhen 518060, China*

(Dated: April 22, 2026)

We study diffusion on multiplex networks with directed interlayer couplings. We demonstrate both numerically and analytically that even with undirected layers, interlayer directionality alone reproduces superdiffusion and the prime regime. We further reveal a new phenomenon, the directionality-induced jamming, whereby directed interlayer links hinder diffusion, fragmenting the system into dynamically disconnected components and preventing convergence to the steady state of the diffusion process. Via an optimization process, we show that this new regime is attainable in both toy models and real-world topologies. These findings underscore the crucial role of interlayer link directionality in shaping the emergent behavior of multiplex systems, with potential implications for the design and control of such systems.

PACS numbers: 89.75.Hc, 89.20.a, 89.75.Kd

Complex systems often exhibit multiple types of interactions operating simultaneously, making network theory [1–8], and in particular, the framework of multilayer and multiplex networks [9–14], an essential tool to describe their structure and dynamics. In a multiplex representation, the same set of nodes is connected through distinct layers, each encoding a different interaction pattern. This architecture captures the intertwined nature of real systems such as social [15–18], transportation [19, 20], and biochemical networks [21–23], where interdependencies between layers give rise to collective behaviors unattainable in single-layer topologies.

Diffusion is among the most fundamental dynamical processes studied in this context. Despite its apparent simplicity, diffusion on multiplex networks reveals a rich phenomenology driven by the interplay between topology and coupling strength. Gómez et al. [24] first showed that interlayer coupling can enhance transport efficiency, leading to *superdiffusion*—a regime where diffusion in the multiplex outpaces that in any individual layer. Since then, extensive efforts have focused on isolating the structural features that promote or hinder its emergence. It has been shown, for instance, that this phenomenon is critically enhanced by the topological dissimilarity between layers [25] and by the misalignment of their spectral eigenvectors [26]. Other structural factors, such as edge overlap, do not determine the onset of superdiffusion but can influence its intensity once the regime is established [27]. Furthermore, the inclusion of long-range interactions has been shown to alter these diffusive time scales [28]. However, most diffusion studies on multiplex assume undirected topologies. Tejedor et al. [29] demonstrated that when directionality within layers is introduced, diffusion can become non-monotonic with coupling, producing the *prime regime*, where intermediate coupling yields the fastest relaxation. Subsequently, Wang et al. [30] proved that the prime regime is fundamentally rooted in the non-normality of the underlying network matrices. These results unveiled how structural asymmetries control diffusion speed, yet the role of directionality in *interlayer* couplings has remained largely unexplored.

In this work, we address this knowledge gap by investigating diffusion on multiplex networks where interlayer links themselves are directed. We demonstrate, both analytically and numerically, that interlayer directionality alone can reproduce all previously known diffusion regimes, including superdiffusion and the prime regime. More importantly, we unveil a new dynamical behavior—directionality-induced jamming—in which the asymmetric orientation of interlayer links suppresses diffusion and dynamically fragments the system into disconnected components, preventing convergence to equilibrium. We further show that this regime can arise not only in synthetic models but also in real-world topologies such as the London transport multiplex [31]. Our findings reveal that interlayer directionality constitutes a fundamental control parameter shaping diffusion in interconnected systems, opening new perspectives for the design, optimization, and robustness analysis of multilayer networks.

We now introduce the notation and framework used to describe diffusion dynamics on multiplex networks with directed interlayer couplings. Consider a two-layer multiplex of N nodes per layer. The state vector representing the concentration on the $2N$ nodes at time t is:

$$\mathbf{x}(t) = (\mathbf{x}_1(t) | \mathbf{x}_2(t))^T \quad (1)$$

The diffusion dynamics in such a system are governed by

$$\frac{d\mathbf{x}^T(t)}{dt} = -\mathbf{x}^T(t)\mathcal{L}, \quad (2)$$

where $\mathcal{L} \in \mathbb{R}^{2N \times 2N}$ is the so-called *supra-Laplacian* matrix, defined for multiplex consisting of two layers as

$$\mathcal{L} = \left(\begin{array}{c|c} D_1 L_1 + D_{12} I_N & -D_{12} I_N \\ \hline -D_{21} I_N & D_2 L_2 + D_{21} I_N \end{array} \right). \quad (3)$$

Here, D_1 and D_2 are the diffusion coefficients within each layer, D_{12} and D_{21} represent interlayer diffusion, L_1 and L_2 are the Laplacian matrices of the respective layers, and I_N denotes the $N \times N$ identity matrix.

We denote by $\{\Lambda_1 \leq \Lambda_2 \leq \dots \leq \Lambda_{2N}\}$ the ordered set of eigenvalues of the supra-Laplacian \mathcal{L} , and by $\{\lambda_1^{(k)} \leq \lambda_2^{(k)} \leq \dots \leq \lambda_N^{(k)}\}$ the eigenvalues of the Laplacian L_k of the k -th layer. In the presence of directionality, eigenvalues are ordered according to their real parts. For a multiplex that forms a strongly connected component, the diffusion dynamics converge to the eigenvector associated with the zero eigenvalue, $\lambda_1 = 0$ (and thus $\Lambda_1 = 0$). This eigenvector corresponds to a uniform concentration distribution across all nodes (e.g., all 1s). The rate of convergence toward this steady state is determined by the real part of the smallest nonzero eigenvalue, λ_2 (or Λ_2 for the multiplex), which governs the slowest relaxation mode of the system.

We now address how directionality can be incorporated into the interlayer coupling. Two distinct mechanisms are considered: *topological directionality* and *induced directionality*. In the first case, directionality is encoded explicitly in the interlayer topology: the presence of a link from node $n_i^{(k)}$ in layer k to its counterpart $n_i^{(l)}$ in layer l does not require the reciprocal link from $n_i^{(l)}$ to $n_i^{(k)}$. The supra-adjacency matrix of such a multiplex can therefore be written as

$$\tilde{A} = \begin{pmatrix} A_1 & \Delta_{12} \\ \Delta_{21} & A_2 \end{pmatrix} \in \mathbb{R}^{2N \times 2N}, \quad (4)$$

where A_k denotes the adjacency matrix of layer $k \in \{1, 2\}$ (assumed symmetric here), and Δ_k is a diagonal matrix whose element $(\Delta_{kl})_{ii} \in \{0, 1\}$ encodes the existence of an interlayer link from node i in layer k to its replica node i in layer l . Consequently, in Eq. (3), the identity matrices I_N appearing in the interlayer blocks must be replaced by Δ_{12} and Δ_{21} to correctly account for directionality. In contrast, *induced directionality* arises when interlayer links are topologically undirected but exhibit asymmetric diffusion coefficients. Retaining the structure of Eq. (3) while imposing $D_{12} \neq D_{21}$

introduces an effective directionality in the coupling between layers, and thus in the overall diffusion dynamics.

In the following, we characterize the effects of interlayer directionality on diffusion dynamics, combining analytical derivations with numerical experiments. We first examine the case of induced directionality, where asymmetry arises solely from unequal interlayer diffusion coefficients ($D_{12} \neq D_{21}$), and subsequently address topological directionality, where the interlayer structure itself imposes directed connectivity. This separation allows us to isolate the distinct physical mechanisms by which interlayer orientation shapes the emergent dynamical regimes of multiplex systems.

We first consider the case where directionality is introduced through asymmetric interlayer diffusion coefficients. In this setting, the supra-Laplacian takes the form

$$\mathcal{L} = \begin{pmatrix} L_1 & 0 \\ 0 & L_2 \end{pmatrix} + D_{12} \begin{pmatrix} I & -I \\ 0 & 0 \end{pmatrix} + D_{21} \begin{pmatrix} 0 & 0 \\ -I & I \end{pmatrix}. \quad (5)$$

Without loss of generality, we set $D_1 = D_2 = 1$ to simplify notation. Since our focus is on the effect of interlayer coupling, it is convenient to work in the basis $(\mathbf{1}|\mathbf{1})^T$ and $(-\mathbf{1}|\mathbf{1})^T$, corresponding to the eigenvectors of the coupling matrices. In this representation, the transformed supra-Laplacian reads

$$\begin{aligned} \hat{\mathcal{L}} &= U\mathcal{L}U^{-1} = \frac{1}{\sqrt{2}} \begin{pmatrix} 1 & 1 \\ -1 & 1 \end{pmatrix} \mathcal{L} \begin{pmatrix} 1 & -1 \\ 1 & 1 \end{pmatrix} \frac{1}{\sqrt{2}} = \\ &= \begin{pmatrix} L_+ & L_- + (D_{21} - D_{12})I \\ L_- & L_+ + (D_{12} + D_{21})I \end{pmatrix}, \end{aligned} \quad (6)$$

where $L_+ = \frac{1}{2}(L_1 + L_2)$ and $L_- = \frac{1}{2}(L_2 - L_1)$, with eigenvalues $\lambda_j^{(+)}$ and $\lambda_j^{(-)}$, respectively. Applying the Schur complement [32] to $|\hat{\mathcal{L}} - \Lambda I| = 0$ yields

$$|L_+ + (D_{12} + D_{21})I - \Lambda I| |L_+ - \Lambda I - (L_- + (D_{21} - D_{12})I)(L_+ + (D_{12} + D_{21})I - \Lambda I)^{-1}L_-| = 0. \quad (7)$$

From Eq. (7), two asymptotic regimes follow:

1. For $D_{12} \gg D_{21}$, $D_{12} \gg 1$ (or more strictly, $D_{12} \gg N$, see the Supplementary Materials for more details), the equation reduces to $|L_+ + D_{12}I - \Lambda I| \cdot |L_2 - \Lambda I| = 0$ and the spectrum separates into eigenvalues scaling with D_{12} and those converging to the eigenvalues of L_2 . The smallest nonzero eigenvalue Λ_2 thus approaches $\lambda_2^{(2)}$, and the slower layer (layer 2) controls the overall convergence rate.
2. Conversely, for $D_{21} \gg D_{12}$, $D_{21} \gg 1$ (again see Supplementary Material for the details of the more stricter condition $D_{21} \gg N$), the equation becomes

$|L_+ + D_{21}I - \Lambda I| \cdot |L_1 - \Lambda I| = 0$ and the situation reverses: $\Lambda_2 \rightarrow \lambda_2^{(1)}$, and diffusion is dictated by layer 1.

The existence of these two limiting cases and because the eigenvalues vary continuously with D_{12} and D_{21} [33] directly imply that the system must transition smoothly between such regimes, passing through the symmetric case $D_{12} = D_{21}$ studied in Ref. [24], where $\Lambda_2 = \lambda_2^{(+)}$. Moreover, if $\lambda_2^{(+)} > \max(\lambda_2^{(1)}, \lambda_2^{(2)})$, Λ_2 would exhibit non-monotonic behavior, which ensures the existence of the prime regime as well. Consequently, induced directionality can reproduce both *superdiffusion* and the *prime regime* reported in previous works [29, 30]. The numerical validation of these regimes for the network described in the Supplementary Material is shown

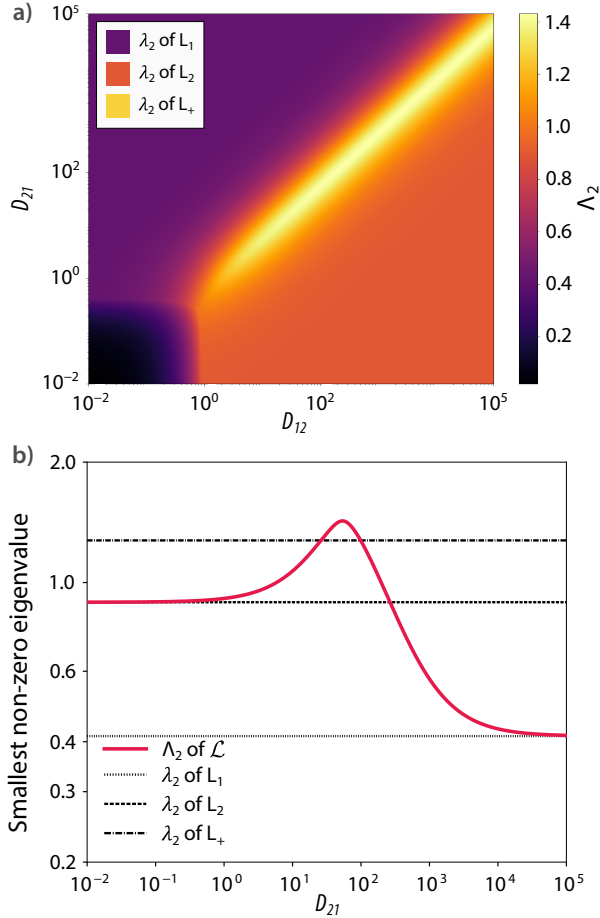


FIG. 1: **Diffusion Dynamics in multiplex networks with induced interlayer directionality.** a) Heat map of the smallest non-zero eigenvalue of \mathcal{L} , Λ_2 , as a function of the coupling parameters D_{12} and D_{21} . b) Evolution of Λ_2 as function of D_{21} when $D_{12} = 100.0$. The network is given in the Supplementary Materials.

in Fig. 1.

We now turn to the case where directionality is encoded explicitly in the interlayer topology. As defined in Eq. (4), the off-diagonal blocks of the supra-Adjacency matrix are non-symmetric, reflecting that the interlayer connection from layer k to layer l does not necessarily imply its reciprocal. Assuming $D_{12} = D_{21} = D_X$ and $D_1 = D_2 = 1$ for simplicity, the supra-Laplacian reads

$$\mathcal{L} = \begin{pmatrix} L_1 & 0 \\ 0 & L_2 \end{pmatrix} + D_X \begin{pmatrix} \Delta_{12} & -\Delta_{12} \\ -\Delta_{21} & \Delta_{21} \end{pmatrix}. \quad (8)$$

For $D_X = 0$, the eigenvalue spectrum of \mathcal{L} is simply the union of the spectra of L_1 and L_2 . To understand how coupling modifies this spectrum, we analyze the weak and strong coupling limits.

Weak coupling ($D_X \rightarrow 0$). In this limit, the interlayer term acts as a perturbation to the block-diagonal matrix $\mathcal{L}_0 = \text{diag}(L_1, L_2)$. Because both L_1 and L_2 are Laplacians, \mathcal{L}_0

possesses a degenerate zero eigenvalue of minimum multiplicity $g_0 = 2$. The first-order correction to the degenerate eigenvalues, $\Lambda^g(1)$, can be expressed as:

$$\Lambda^g(1) = \Lambda^g(0) + \mu_g D_X + o(D_X) \quad (9)$$

where $g = \{1, \dots, g_0\}$, $\Lambda^g(0)$ is the unperturbed eigenvalue (here, $\Lambda^g(0) = 0$), and μ_g are the eigenvalues of the perturbation matrix $W \in \mathbb{C}^{g_0 \times g_0}$ whose elements are given by $W_{kl} = v_k^T \mathcal{D} v_l$. Since the eigenvectors v_i that span the kernel of \mathcal{L}_0 are $(\mathbf{1}|\mathbf{0})^T$ and $(\mathbf{0}|\mathbf{1})^T$, the explicit construction of W yields

$$W = \frac{1}{N} \begin{pmatrix} \sum_{i=1}^N (\Delta_{12})_{ii} & -\sum_{i=1}^N (\Delta_{12})_{ii} \\ -\sum_{i=1}^N (\Delta_{21})_{ii} & \sum_{i=1}^N (\Delta_{21})_{ii} \end{pmatrix}. \quad (10)$$

whose eigenvalues are $\mu_1 = 0$ and $\mu_2 = N^{-1} \sum_i [(\Delta_{12})_{ii} + (\Delta_{21})_{ii}]$. Consequently, the smallest nonzero eigenvalue of \mathcal{L} grows linearly with the coupling as

$$\Lambda_2 = \mu_2 D_X + o(D_X). \quad (11)$$

indicating that for weak coupling, the relaxation rate increases linearly with D_X , proportional to the sum of interlinks.

Strong coupling ($D_X \rightarrow \infty$). In the opposite limit, we analyze the characteristic polynomial $|\hat{\mathcal{L}} - \Lambda I| = 0$ in the transformed basis used in Eq. (6). This yields

$$\begin{vmatrix} L_+ - \Lambda I & L_- + D_X \Delta_- \\ L_- & L_+ + D_X \Delta_+ - \Lambda I \end{vmatrix} =$$

$$|L_+ + D_X \Delta_+ - \Lambda I| \cdot$$

$$|L_+ - \Lambda I - (L_- + D_X \Delta_-)(L_+ + D_X \Delta_+ - \Lambda I)^{-1} L_-| = 0 \quad (12)$$

where $\Delta_+ = (\Delta_{12} + \Delta_{21})$ and $\Delta_- = (\Delta_{21} - \Delta_{12})$. The first term, $|L_+ + D_X \Delta_+ - \Lambda I|$, produces eigenvalues that diverge linearly with D_X , with slopes set by the diagonal entries of Δ_+ , which can be 1 or 2 (note that the cases with zero value for Δ_+ are not considered, so Δ_+^{-1} is well defined). The second factor, $|L_+ - \Lambda I - (L_- + D_X \Delta_-)(L_+ + D_X \Delta_+ - \Lambda I)^{-1} L_-|$, is more intricate. In the asymptotic limit $D_X \rightarrow \infty$, assuming Δ_+ is invertible, this term converges to $|L_+ - \Delta_- \Delta_+^{-1} L_- - \Lambda I|$. This indicates that the second set of eigenvalues, $\lambda_i^{(\pm)}$, with $i = 1, \dots, N$, converges to the spectrum of the matrix $L_+ - \Delta_- \Delta_+^{-1} L_-$, which is Hermitian, hence, its eigenvalues are real and finite. Additionally, it can be proven that $0 \leq \lambda_i^{(\pm)} \leq \lambda_{\max}(L_+) - \lambda_{N-i+1}(\Delta_- \Delta_+^{-1} L_-)$ (see Supplementary Materials for the proof).

A key consequence is that the zero eigenvalue can recover a degeneracy of two or higher at arbitrarily large values of D_X , implying the emergence of a new regime in which diffusion effectively stalls. In this *directionality-induced jamming* regime, the system becomes dynamically partitioned into disconnected components, preventing convergence to a uniform steady state. Admittedly, the convergence rate to the finite

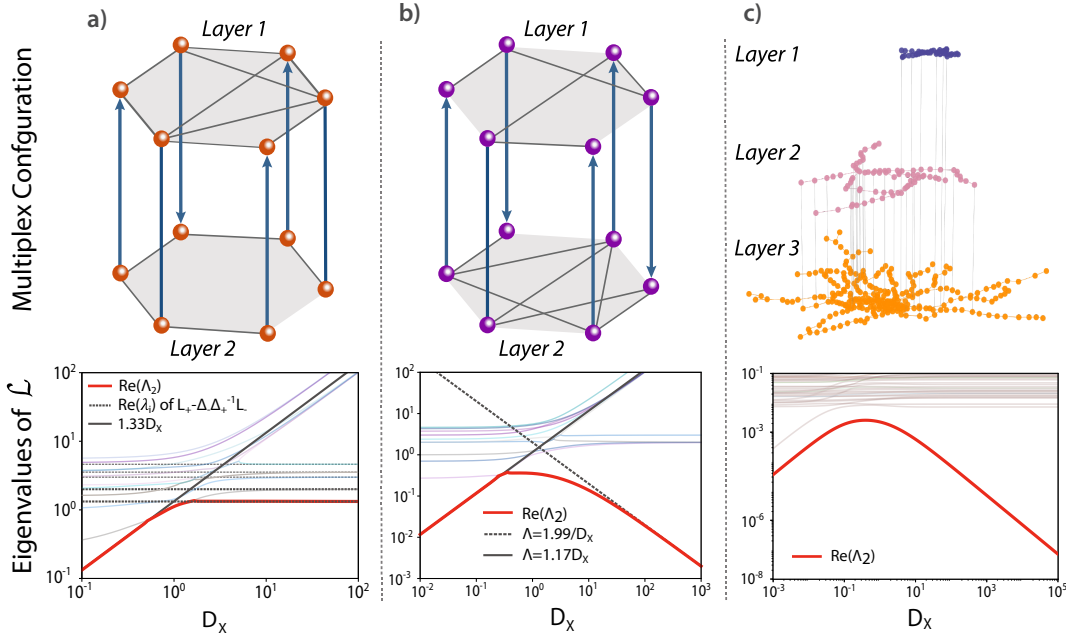


FIG. 2: **Diffusion Dynamics in multiplex networks with topological interlayer directionality.** Evolution of the eigenvalues of \mathcal{L} versus the coupling parameter D_X for different network configurations: a) and b) are synthetic networks of $N = 6$ nodes per layer. c) represents the London transport network [31], where the nodes are the stations and the links are the connections between them. Layer 1 represents the DLR line, layer 2 the overground, and layer 3 the underground. It is assumed that $D_K = 1.0$ for all layers of any configuration.

eigenvalues can be determined through perturbation analysis. By rewriting \mathcal{L} as follows, with $\epsilon = 1/D_X$:

$$\mathcal{L} = D_X(\mathcal{D} + \epsilon\mathcal{L}_0) = D_X \left[\begin{pmatrix} \Delta_{12} & -\Delta_{12} \\ -\Delta_{21} & \Delta_{21} \end{pmatrix} + \epsilon \begin{pmatrix} L_1 & 0 \\ 0 & L_2 \end{pmatrix} \right] \quad (13)$$

we can treat $\epsilon\mathcal{L}_0$ as a perturbation of \mathcal{D} . In this case, the first-order expansion for the eigenvalue Λ_2 , (whose unperturbed value $\Lambda_2(0) = 0$) yields

$$\Lambda_2 = D_X [\Lambda_2(0) + \epsilon\mu_2 + \mathcal{O}(\epsilon^2)] = \mathcal{O}(1/D_X). \quad (14)$$

That is, Λ_2 decreases at a rate of at least D_X^{-1} .

Figure 2 illustrates these effects for the synthetic topology depicted in Fig. 2a,b, here used as an illustrative example. However, to fully understand this new behavior, it is necessary to identify the underlying mechanism. It can be shown [34] that, in an equivalent form, the effective Laplacian matrix, under strong-coupling conditions, can be expressed as

$$L_{\text{eff}} = \Delta_+^{-1}(\Delta_{21}L_1 + \Delta_{12}L_2) \quad (15)$$

This expression shows explicitly that the intra-layer connectivity of node i in a given layer is preserved in the strong-coupling projection if and only if there exists one directed inter-layer link connecting its replica node in the other layer to that node. When this condition is violated due to strict topological directionality (zero-weight inter-layer links), the corresponding intra-layer links become dynamically inactive,

leading to an effective deletion of paths in the projected network. The accumulation of such local suppressions produces dynamically disconnected components, which constitute the microscopic origin of the jamming regime. Within this framework, it is therefore expected that multiplex systems characterized by sparse layers, low clustering coefficients, or weak edge overlap are generally more prone to entering the jamming regime, as such macroscopic features increase the likelihood of fragmentation with the introduction of asymmetric (directed) interlayer connections between replica nodes. However, these structural observables should be regarded as indicative rather than mechanistic.

Furthermore, to explore the generality and potential practical relevance of these findings, we investigate whether it is possible to induce the jamming regime in a real-world system, such as the London transportation system, which has previously been modeled as a multiplex network [31]. Since the network structure is predetermined, we examined the emergence of directionality-induced jamming by introducing subtle structural modifications to the interlayer connectivity. In particular, we considered the problem as an optimization problem via a simulated annealing algorithm, where we selectively pruned and assigned directionality to the interlinks. By exploring this restricted topological space—modifying exclusively the interlayer coupling—we sought configurations that maximize the likelihood of a jamming regime. As shown in Fig. 2c, it is indeed possible to identify interlayer architectures that trigger jamming even within the constraints of real-world

topologies [34].

In summary, we have shown that directionality in the coupling between layers of a multiplex network profoundly alters diffusion dynamics. Through analytical derivations and numerical experiments, we demonstrated that interlayer directionality alone—without any asymmetry within layers—can reproduce both the superdiffusion and prime regimes previously reported for directed multiplexes. More importantly, we uncovered a new dynamical regime, the *directionality-induced jamming* regime, in which strong asymmetric couplings hinder diffusion and dynamically fragment the system into effectively disconnected components. This jamming regime emerges from purely structural asymmetry and is characterized by the vanishing of the smallest nonzero eigenvalue of the supra-Laplacian as $\Lambda_2 \sim D_X^{-1}$. Moreover, the disconnected components might map quite closely to individual layers, but generally involve nodes of different layers, making it difficult to predict a priori the structural or dynamical conditions (e.g., layer topology) under which jamming will occur. Addressing this challenge remains a key open problem that we expect will spur further research.

Finally, our findings identify interlayer directionality as a fundamental control parameter governing transport, relaxation, and connectivity in multiplex systems. Beyond their theoretical relevance, they have direct implications for the design and regulation of interconnected infrastructures—such as transportation and communication networks—, where directionality can be engineered or exploited to either enhance or suppress diffusion. We expect the concept of directionality-induced jamming to stimulate further exploration of how orientation and asymmetry shape collective dynamics (e.g., information or rumor spreading) in complex multilayer systems.

Acknowledgments. Y.M. and A.T. were partially supported by the Government of Aragón, Spain, and “ERDF A way of making Europe” through grant E36-23R (FENOL), and by Ministerio de Ciencia, Innovación y Universidades, Agencia Española de Investigación (MICIU/AEI/10.13039/501100011033) Grant No. PID2023-149409NB-I00. A.T. was also partially supported by NSF Grants EAR-2342937, RISE-2425932, and RISE-2425748.

* alej.tejedor@gmail.com

† xiangrong.wang@outlook.com

‡ yamir.moreno@gmail.com

- [1] D. J. Watts and S. H. Strogatz, *Nature* **393**, 440 (1998).
- [2] A.-L. Barabási and R. Albert, *Science* **286**, 509 (1999), <http://science.sciencemag.org/content/286/5439/509.full.pdf>.
- [3] M. Newman, *Networks: An Introduction* (Oxford University Press, Inc., New York, NY, USA, 2010).
- [4] S. Boccaletti, V. Latora, Y. Moreno, M. Chavez, and D.-U. Hwang, *Physics Reports* **424**, 175 (2006).
- [5] A. Barrat, M. Barthélemy, and A. Vespignani, *Dynamical Processes on Complex Networks*, 1st ed. (Cambridge University Press, New York, NY, USA, 2008).
- [6] I. Rodríguez-Iturbe and A. Rinaldo, *Fractal River Basins: Chance and Self-Organization*, 2nd ed (Cambridge Univ Press, New York, 2001) p. 547.
- [7] E. Bullmore and O. Sporns, *Nature Reviews Neuroscience* **10**, 186 (2009).
- [8] A. Tejedor, A. Longjas, D. Edmonds, T. Georgiou, I. Zaliapin, A. Rinaldo, and E. Fofoula-Georgiou, *Proc. Natl. Acad. Sci. U.S.A.* (2017).
- [9] S. Boccaletti, G. Bianconi, R. Criado, C. del Genio, J. Gómez-Gardeñes, M. Romance, I. Sendiña Nadal, Z. Wang, and M. Zanin, *Phys. Rep.* **544**, 1 (2014).
- [10] G. Bianconi, *Multilayer Networks: Structure and Function* (Oxford University Press, 2018).
- [11] A. Aleta and Y. Moreno, *Annual Review of Condensed Matter Physics* **10**, 45 (2019).
- [12] M. De Domenico, *Nature Physics* **19**, 1247 (2023).
- [13] M. De Domenico, A. Solé-Ribalta, E. Cozzo, M. Kivelä, Y. Moreno, M. A. Porter, S. Gómez, and A. Arenas, *Phys. Rev. X* **3**, 041022 (2013).
- [14] M. Kivelä, A. Arenas, M. Barthélemy, J. P. Gleeson, Y. Moreno, and M. A. Porter, *J. Complex Netw.* **2**, 203 (2014).
- [15] E. Cozzo, R. A. Baños, S. Meloni, and Y. Moreno, *Phys. Rev. E* **88**, 050801 (2013).
- [16] W. Li, S. Tang, W. Fang, Q. Guo, X. Zhang, and Z. Zheng, *Phys. Rev. E* **92**, 042810 (2015).
- [17] G. F. de Arruda, E. Cozzo, T. P. Peixoto, F. A. Rodrigues, and Y. Moreno, *Phys. Rev. X* **7**, 011014 (2017).
- [18] S. E. Smith-Aguilar, F. Aureli, L. Busia, C. Schaffner, and G. Ramos-Fernández, *Primates* **60**, 277 (2019).
- [19] A. Aleta, S. Meloni, and Y. Moreno, *Scientific Reports* **7**, 44359 (2017).
- [20] A. Tejedor, A. Longjas, P. Passalacqua, Y. Moreno, and E. Fofoula-Georgiou, *Geophysical Research Letters* **45**, 9681.
- [21] E. Cozzo, A. Arenas, and Y. Moreno, *Phys. Rev. E* **86**, 036115 (2012).
- [22] F. Battiston, V. Nicosia, M. Chavez, and V. Latora, *Chaos* **27**, 047404 (2017).
- [23] A. Valdeolivas, L. Tichit, C. Navarro, S. Perrin, G. Odelin, N. Levy, P. Cau, E. Remy, and A. Baudot, *Bioinformatics* **35**, 497 (2018).
- [24] S. Gómez, A. Díaz-Guilera, J. Gómez-Gardeñes, C. J. Pérez-Vicente, Y. Moreno, and A. Arenas, *Phys. Rev. Lett.* **110**, 028701 (2013).
- [25] A. B. Serrano, J. Gómez-Gardeñes, and R. F. S. Andrade, *Phys. Rev. E* **95**, 052312 (2017).
- [26] H. Liu, S. Dai, J. Zhao, X. Wu, S. Tan, G. Chen, Z. Zeng, and J. Lü, *IEEE Transactions on Systems, Man, and Cybernetics: Systems* **55**, 9043 (2025).
- [27] G. Cencetti and F. Battiston, *New Journal of Physics* **21**, 035006 (2019).
- [28] A. Allen-Perkins, A. B. Serrano, and R. F. S. Andrade, *The European Physical Journal B* **97**, 88 (2024).
- [29] A. Tejedor, A. Longjas, E. Fofoula-Georgiou, T. T. Georgiou, and Y. Moreno, *Phys. Rev. X* **8**, 031071 (2018).
- [30] X. Wang, A. Tejedor, Y. Wang, and Y. Moreno, *New Journal of Physics* **23**, 013016 (2021).
- [31] M. De Domenico, A. Solé-Ribalta, S. Gómez, and A. Arenas, *Proc. Natl. Acad. Sci. U.S.A.* **111**, 8351 (2014).
- [32] R. W. Cottle, *Linear Algebra and its Applications* **8**, 189 (1974).
- [33] R. A. Horn and C. R. Johnson, *Matrix Analysis*, 2nd ed. (Cambridge University Press, Cambridge, UK, 2013).
- [34] See Supplemental Material [url] for additional results and details, which includes Ref. [35].

- [35] S. Kirkpatrick, C. D. Gelatt Jr, and M. P. Vecchi, *Science* **220**, 671 (1983).